



# SLHC-PP

## DELIVERABLE REPORT

### EU DELIVERABLE:

---

Document identifier:	<b>SLHC-PP-D6.3.1</b>
Contractual Date of Delivery to the EC	<b>End of Month 36 (March 2011)</b>
Actual Date of Delivery to the EC	<b>30/03/2011</b>
Document date:	<b>30/03/2011</b>
Deliverable Title:	<b>Construction of corrector magnet package</b>
Work package:	<b>WP6: Development of Nb-Ti quadrupole magnet prototype</b>
Lead Beneficiary:	<b>CIEMAT</b>
Authors:	<b>F. Aragon, J. Calero, J. Gama, J.L. Gutierrez, T. Martinez, E. Rodriguez, I. Rodriguez, L. Sanchez, F. Toral, C. Vazquez (CIEMAT), M. Karppinen, S. Russenschuck, D. Smekens (CERN), A. Brummit, M. Courthold (STFC)</b>
Document status:	<b>Released</b>
Document link:	<a href="https://edms.cern.ch/document/1093308/1">https://edms.cern.ch/document/1093308/1</a>

---



## DELIVERABLE REPORT

Doc. Identifier:  
SLHC-PP-D6.3.1

Date: 30/03/2011

### History of Changes

Version	Date	Comment	Authors

Copyright notice:

Copyright © Members of the SLHC-PP Collaboration, 2009.

For more information on SLHC-PP, its partners and contributors please see [www.cern.ch/SLHC-PP/](http://www.cern.ch/SLHC-PP/)

The Preparatory Phase of the Large Hadron Collider upgrade (SLHC-PP) is a project co-funded by the European Commission in its 7th Framework Programme under the Grant Agreement n° 212114. SLHC-PP began in April 2008 and will run for 3 years.

The information contained in this document reflects only the author's views and the Community is not liable for any use that may be made of the information contained therein.



# DELIVERABLE REPORT

Doc. Identifier:  
SLHC-PP-D6.3.1

Date: 30/03/2011

## TABLE OF CONTENTS

1. EXECUTIVE SUMMARY .....	4
2. DESIGN WORK, PROCUREMENT, MODEL CONSTRUCTION, AND COLLARING TEST FOR MCXB AT CERN.....	5
3. ENGINEERING DESIGN AND CONSTRUCTION WORK ON THE SEXTUPOLE AND OCTUPOLE AT CIEMAT.....	17
4. ENGINEERING DESIGN FOR THE SKEW QUADRUPOLE.....	29
5. CONCLUSIONS .....	34

## 1. EXECUTIVE SUMMARY

For the triplets of the LHC upgrade phase 1, it was foreseen to group corrector magnets in a dedicated cryo-assembly, the so-called corrector package (CP) [1]. This corrector package contains horizontal and vertical orbit correctors (MCXB), a skew-quadrupole (MQXS), and higher-order multipole correctors. The MQXS magnets are constructed in a similar way as the MCXB dipoles. The single-layer coils are wound with the same cable as the MCXB and the turns are grouped in 2 winding blocks.

The correction of the higher order field imperfections of the triplet quadrupoles and the separation dipole magnets will require local correctors of the same multipole order as in the LHC. The strength requirements are 0.055 Tm at 40 mm reference radius for the sextupole corrector (MCSX) and 0.035 Tm at 40 mm for the octupole corrector MCOX. The baseline requirements for the higher order correctors can be met with a super-ferric design with a pole gap of 140 mm. The simple racetrack coils are wound with single, enameled superconducting wire and are impregnated with epoxy or with more radiation-hard, cyanate-ester resin. The advantage of super-ferric magnets is that the coils are located at a larger radius from the bore, which reduces the radiation dose on the coil. The study of the Phase-I upgrade of the LHC insertion regions around the IP1 and IP5 propose the corrector magnets be grouped in a dedicated cryo-assembly, denoted Corrector Package (CP). This Corrector Package contains horizontal and vertical orbit correctors (MCXB), skew-quadrupole (MQXS), and higher-order multipole correctors. In addition, a pair of MCXB magnets will be installed in the Q2 cryo-assemblies.

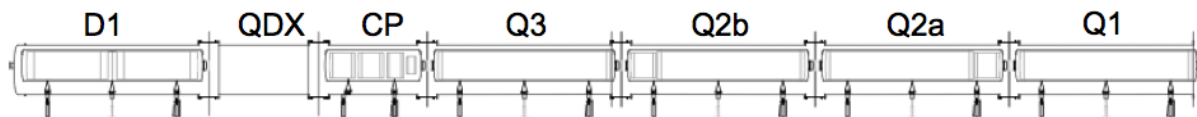


Fig. 1: LHC IR region layout for D1, the corrector package (CP) and Inner Triplet Quadrupoles Q1-Q3.

Studies of magnet protection from particle debris have shown that the energy deposition in the corrector package is generally higher than in the MQXC triplet quadrupoles, and that the radiation dose can be reduced by a factor of two, if the aperture of the correctors is increased from 120 to 140 mm in diameter. By adding a 10-mm-thick stainless steel shielding between the beam tube and the coils, the dose can be reduced by a factor 3 resulting in a maximum dose of about 10 MGy. The dose is calculated for the lifetime of the LHC IR Upgrade Phase 1, which in terms of integrated luminosity is estimated at  $1000 \text{ fb}^{-1}$ . All materials used for magnet construction must comply with the doses. All correctors have a coil aperture or equivalent pole gap of 140 mm.

The assembly of the corrector package and Q2 cold masses and cryostats will be carried out at CERN. The alignment of the magnets and welding of the stainless steel half-shells, which make up the helium vessel, need specific features in the magnet yoke, common to the MQXC quadrupoles and to the correctors. The iron yoke laminations of the MCXB and MQSX magnets also have the same features for routing the busbars and the heat exchangers as the MQXC quadrupoles [3]. The correction of the higher order field imperfections of the triplet quadrupoles and the separation dipole magnets require local

correctors of the same multipole order as in the LHC. The strength requirements are summarized in Table 1.

Magnet Type	Current	Integrated Strength (Rref = 40 mm)	Aperture
MCXB (B1/A1)	+/- 2.4 kA	1.5 Tm	140 mm
MQXS (A2)	+/- 2.4 kA	0.65 Tm	
MCXS (B3)	+/- 120 A	0.055 Tm	
MCXSS (A3)	+/- 120 A	0.055 Tm	
MCXO (B4)	+/- 120 A	0.035 Tm	
MCXSO (A4)	+/- 120 A	0.035 Tm	
MCXT (B6)	+/- 600 A	0.075 Tm	

Table 1: Parameters of the Corrector Package Magnets

After the re-scoping of the WP-6 in spring of 2010, it was decided to concentrate on magnet design and manufacture of magnet types with novel features. The conceptual design of the MCXB magnet was completed at CERN, while the superferric sextupole magnet was constructed at CIEMAT. The design and procurement of components for the octupole magnet has also advanced to a stage where assembly work can start.

## 2. DESIGN WORK, PROCUREMENT, MODEL CONSTRUCTION, AND COLLARING TEST FOR MCXB AT CERN

The MCXB orbit correctors are used to correct the misalignment of the MQXC quadrupoles and to adjust the crossing angle and position of the two beams at the interaction point. The goal of the orbit correction is to control the orbit at least down to the level of the BPM resolution and to provide sufficient strength to avoid frequent re-alignment of the inner triplets. In addition, the inner triplet orbit correction scheme shall be as local as possible to minimize the use of the orbit correctors in the Matching Sections and hence preserving the flexibility of the crossing schemes. The present baseline layout of the triplets includes two pairs of identical (except for the 90 deg. rotation), individually powered dipoles for correction in the horizontal and vertical planes. One pair is located in the corrector package, while the magnets of the other pair are located at the extremities of the Q2 coldmass. To meet the goals of the orbit correction scheme, it has been proposed the latter ones be combined horizontal/vertical correctors, in a nested construction because of space constraints. Using such a combined magnet also in the corrector package would contribute to the minimization of the D1-IP distance, hence reducing the number of parasitic beam-beam collisions.

### 2.1. THE MCXB MODEL PROGRAM

The model program includes the development and the testing of 3 variants of MCXB dipoles:

1. Single layer dipole with porous polyimide insulation (baseline).
2. Single layer dipole with vacuum impregnated coils and glass insulation.
3. Feasibility study and development of a combined H/V-corrector (nested coils).

The goal of the first two phases is to gain experience with the new cable and to measure the mechanical characteristics of such coils. Cold testing of the model magnets will allow the comparison of these two technologies in the same mechanical structure and, therefore, give valuable insight of possible performance limitations. The coils of the first two models can then serve as the first layer of the model H/V corrector.

**2.2. CONCEPTUAL DESIGN**

In the initial layout of the new Inner Triplets (2008), the MCXB dipole correctors had a design strength of 6 Tm, for an aperture of 140 mm and a total length of 1.9 m. The initial design foresaw collared coils using a newly developed Rutherford-type cable. In 2009, the requirements changed for shorter magnets (< 1 m) with single layer coil and integrated strength of 1.5 Tm at a current of 2.4 kA, corresponding to a 70 µrad kick of the 7 TeV proton beam.

Integrated field	1.5	Tm	(6 Tm)
Nominal field	2.28	T	(4 T)
Magnetic length	0.65	m	(1.5 m)
Nominal current	2400	A	(2438 A)
Stored energy	28	kJ	(233 kJ)
Self inductance	10	mH	(78 mH)
Working point	50	%	(60 %)
Cable width	4.37 mm		
Cable mid-height	0.845 mm		
Total length	975	mm	(1.9 m)
Aperture	140	mm	(140 mm)
Total mass	1350	kg	(2750 kg)

Table 2 - MCXB design parameters

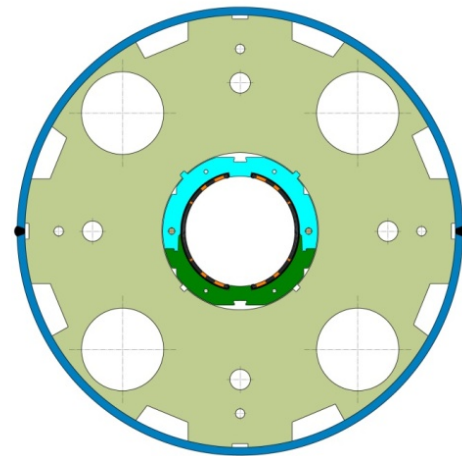


Figure 2: MCXB Magnet cross section

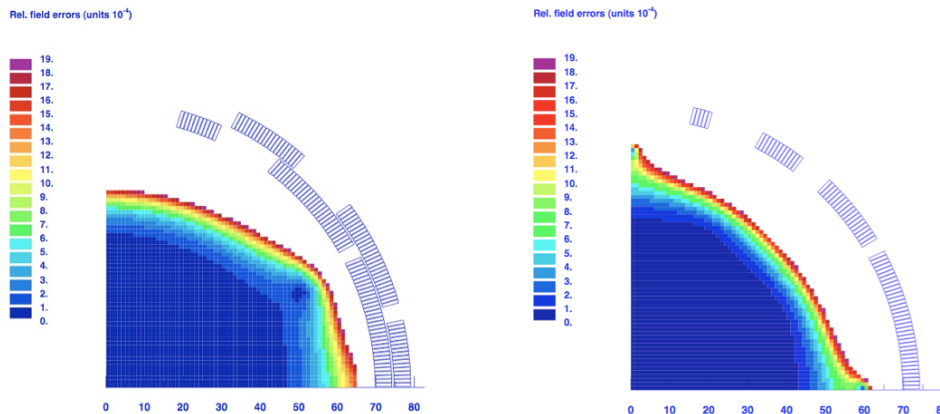


Figure 3: MCXB 2D Field Quality: 6 Tm, 6-block design and the actual 1.5 Tm 4-block, single layer design.

### 2.3. MAGNETIC DESIGN OF THE 1.5 TM MCXB (4 BLOCKS DESIGN)

The magnetic design (2D and 3D) has been carried out at CERN, using the field computation program ROXIE [6]. The 72 turns of the single-layer coil are grouped in 4 winding blocks of 36, 19, 12, and 5 turns. The first block is split in two at coil ends for magnetic field optimization and to ease the coil winding.

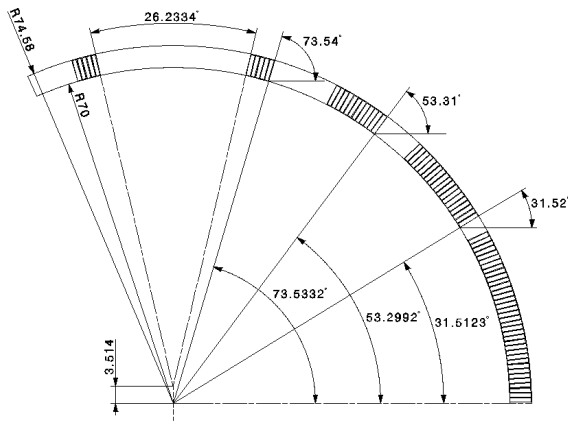


Figure 4: MCXB Coil Cross-Section



Figure 5: 3D view of the 855-mm-long MCXB coil

Contribution to $B_1$	Length	Integrated Field
Straight section	336 mm	0.766 Tm
Return End	250 mm	0.37 Tm
Lead End	250 mm	0.37 Tm
Total	836 mm	1.51 Tm
(with end spacers)	855 mm	

Table 3: MCXB Dipole, main field distribution

3D Harmonics at 2.4 kA (units)			
$B_1$	1.51 Tm	$a_1$	-22.71
$b_3$	0.20	$a_3$	6.32
$b_5$	-3.59	$a_5$	-0.52
$b_7$	-4.46	$a_7$	-0.07
$b_9$	-0.84	$a_9$	0.03
$b_{11}$	-0.41	$a_{11}$	-0.02

Table 4: MCXB Dipole Field quality

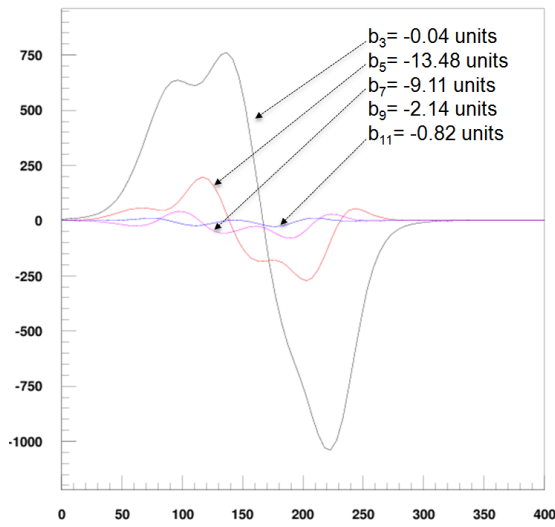


Figure 6: 3D computation of field harmonics (MCXB Coil Return End)

The limited stored energy in the magnet allows for a relatively simple quench protection scheme. Simulations (see Fig. 9) have shown that an energy extraction system based on a warm by-pass diode and a  $0.16 \Omega$  dump resistor is sufficient to protect the magnet. No quench heaters are required.

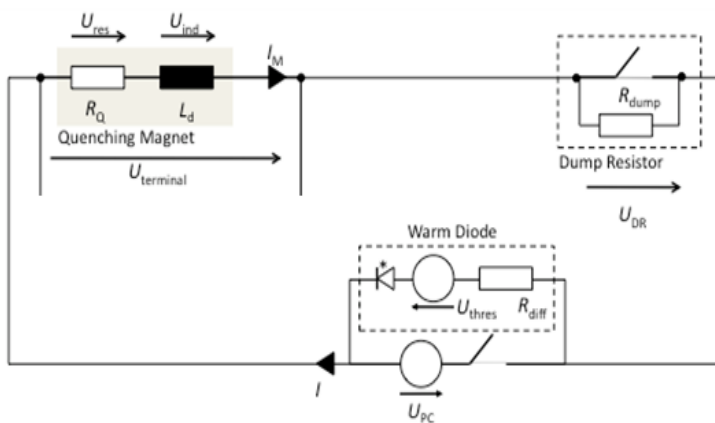


Figure 7: MCXB Energy extraction scheme

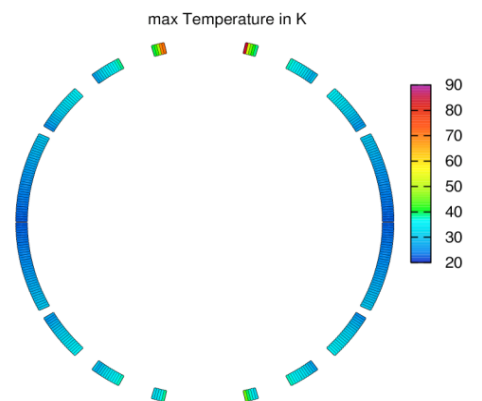


Figure 8: Temperature profile during quench

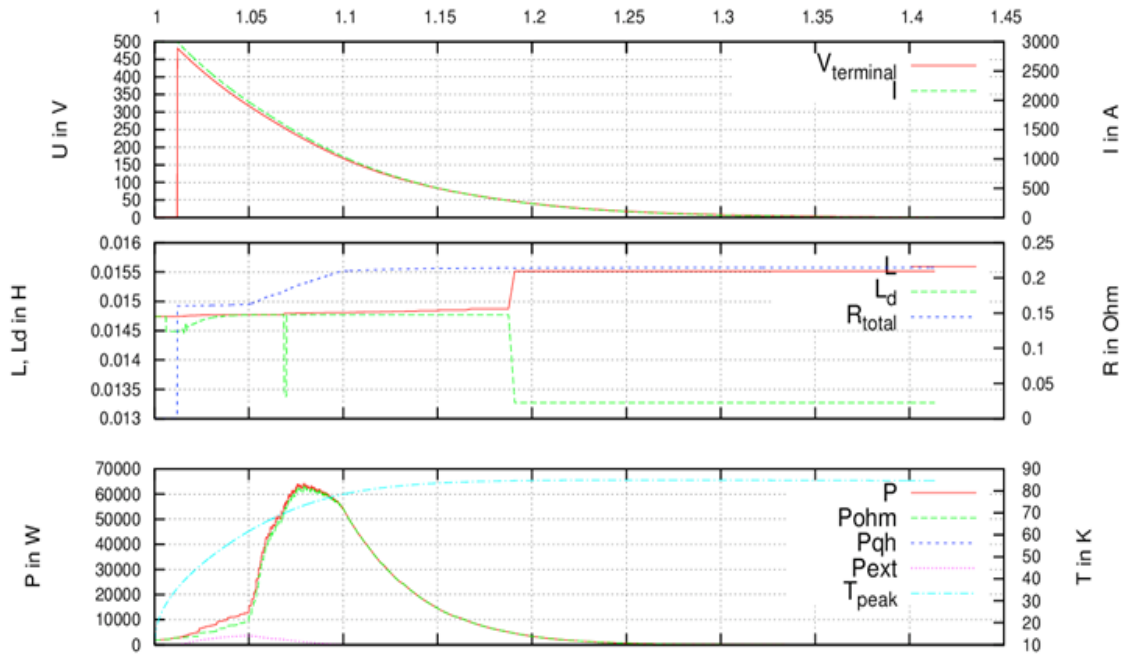


Figure 9: MCXB Quench Computation; voltage, inductance, and power dissipation

Structural Analysis of the MCXB model has been carried out at CERN using ANSYS® [5]. The 2D cross-section of the collared coils was used to assess the deformation and stress in the collars, as well as the evolution of the azimuthal compression in the coil during collaring, cool down, and when the magnet is powered.

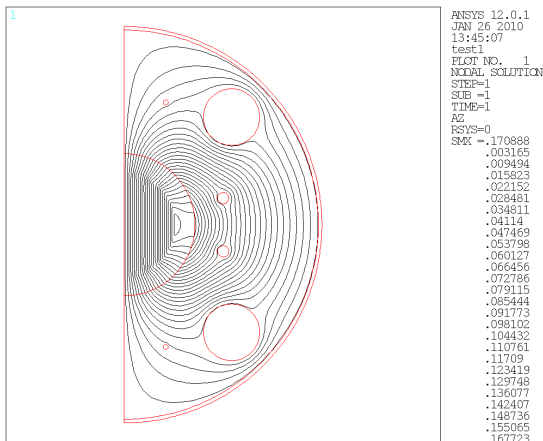


Figure 10: ANSYS magnetic analysis, flux lines

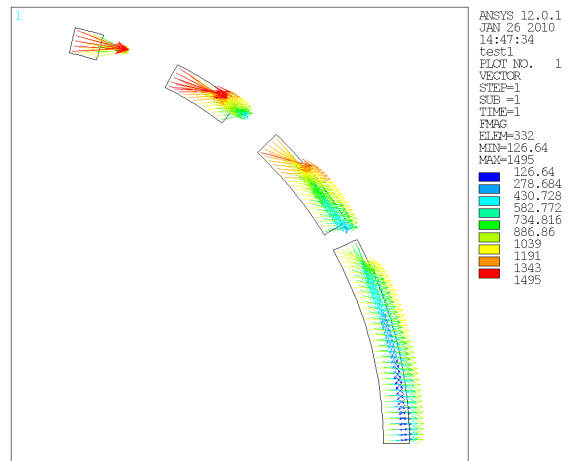


Figure 11: ANSYS magnetic analysis, force vectors in the coil

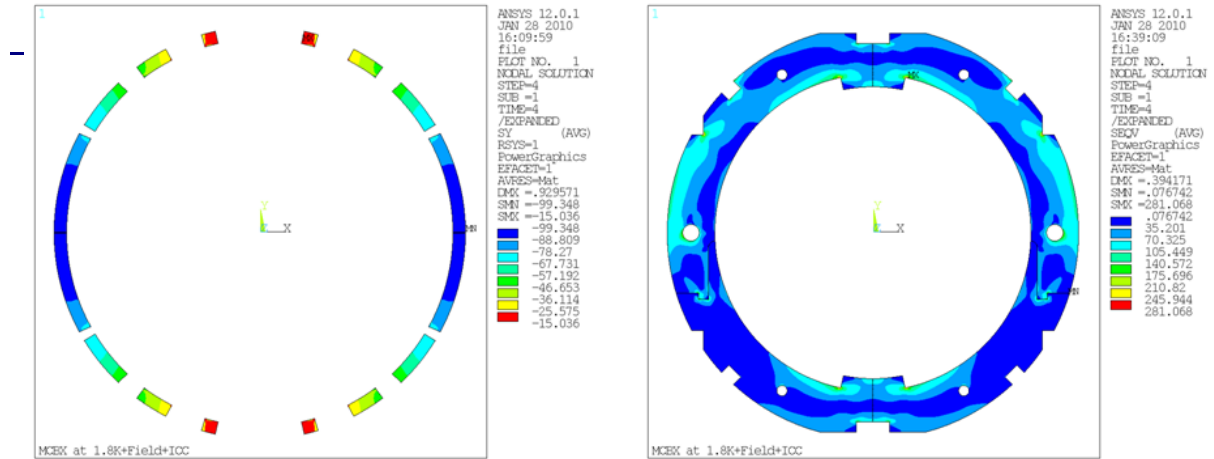


Figure 12: Left: Field distribution in the coil. Right: Stress distribution in the collar

The electro-magnetic simulation in Ansys® agrees well with the ROXIE results. Under magnetic forces the azimuthal compression of the coils decreases at the pole, and increases at the mid-plane.

#### 2.4. DEVELOPMENT OF THE 18-STRAND RUTHERFORD CABLE FOR MCXB DIPOLE CORRECTORS

The new 18-strand cable is based on the LHC strand type 5 to make use of the existing stock of some 270 km from the LHC production. The cable is wound with a transposition pitch of 33 mm, a width of 4.37 mm, and a mid-thickness of 0.845 mm. The small size of the cable required modification of the cabling machine to allow a precise control of the geometry and accurate measurement of this geometry. A total of 1.5 km of cable was produced mid 2010 for the MCXB model program

Strand Parameters			Cable Parameters		
Cu:Sc	1.75		No of strands	18	
Strand diam.	0.48	mm	Metal Area	3.257	mm <sup>2</sup>
Metal Section	0.181	mm <sup>2</sup>	Cable Thickness	0.845	mm
No of filaments	2300		Cable Width	4.370	mm
Filaments diam.	6.0	µm	Cable Area	3.692	mm <sup>2</sup>
I (5T,4.2K)	203	A	Metal fraction	0.882	
Jc	3085	A/ mm <sup>2</sup>	Keystone angle	0.67	°
			Inner Thickness	0.819	mm
			Outer thickness	0.870	mm

Table 5: Parameters of the 18 strand NbTi cable for MCXB and MQXS magnets



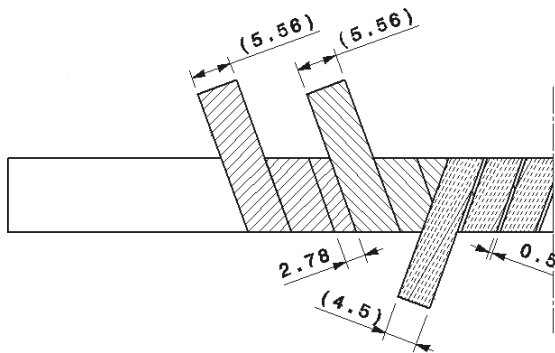


Figure 15: Porous Polyimide Insulation wrapping scheme

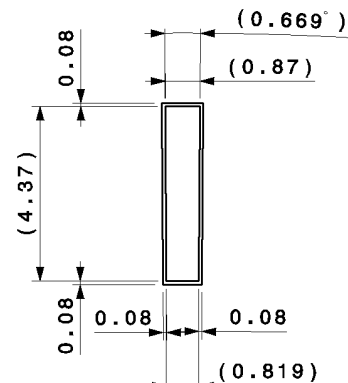


Figure 16: Insulated 18-strand cable cross-section. Dimensions under compressed state (at 80 MPa)

The 55- $\mu\text{m}$ -thick tape with b-stage polyimide resin is a specific product (PIXEO) that was manufactured by Kaneka Corporation Japan. During the LHC magnet production, very large batches of PIXEO were manufactured for CERN. After the completion of the LHC magnet production the fabrication of the PIXEO grade was discontinued and this product is no longer available on the market. A new partnership started in early 2009 with Kaneka Texas to restart the production of industrial quality PIXEO grade. After 2 years of development and testing, the latest results are encouraging. If successful, these developments should allow Kaneka Texas to be in position to produce PIXEO films and tapes in small to large quantities, in various sizes and coating thicknesses.

## 2.6. CHARACTERIZATION OF THE 18-STRAND CABLE WITH POROUS INSULATION (YOUNG'S MODULUS & DIELECTRIC PROPERTIES)

The electrical insulation is ensured by the first two layers of 25-micron-thick plain polyimide tapes. This is the minimum thickness reasonably achievable below which the film becomes too fragile and is easily punctured or broken during the cable wrapping during the coil winding. The 55  $\mu\text{m}$  PIXEO tape is also the smallest tape available. Under compressed state, the 80  $\mu\text{m}$  insulation thickness still represents 16% of the total cable thickness, compared to 10% in the case of the LHC dipoles (inner layer), results in relatively low coil modulus. Tests carried out at CERN and at STFC/RAL on straight stacks of cables have shown that the expected young modulus for the MCXB cable is around 6 GPa at room temperature.

This will be confirmed using a specific press to measure the elastic modulus of the entire MCXB coil. Further investigations are still required to measure accurately the mechanical properties of the coils to gain experience with this new cable. Dielectric tests showed a breakdown voltage between turns at room temperature in air to be higher than 2.5 kV DC.

A test campaign has been completed at STFC/RAL with series of cured straight stacks to determine the creep behaviour, the young's modulus (at 293 K and at 77 K) and the dielectric properties of the insulation on unloaded samples and under compression.

## 2.7. COIL AND COLLAR DESIGN FOR THE SINGLE LAYER MCXB CORRECTOR DIPOLE

The 72 turns of the single-layer coil are grouped in four winding blocks. The coils are clamped with stand-alone collars made of 2-mm-thick austenitic steel (316LN). The choice of 316LN steel is based on the availability of this product in flat sheets, which facilitates the production of collars by EDM. Collars for the short mechanical model have been delivered. For the series production of the MCXB, the collars could be produced by punching, making

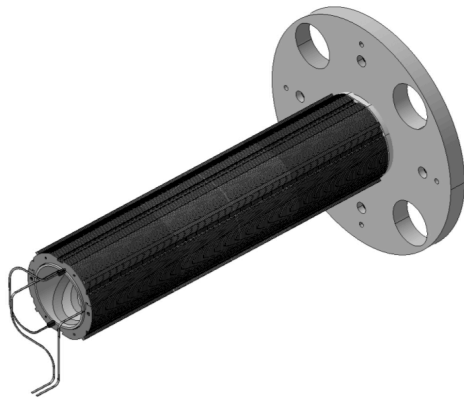


Figure 17: MCXB collared coils, with end plates in the backplane and the coil terminals routing at the front plane (front end plates not shown)

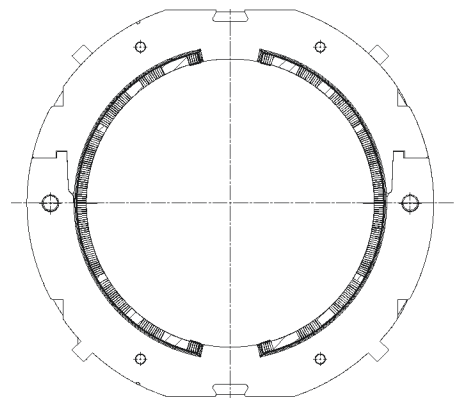


Figure 18: MCXB Collared Coil Cross-section

use of the remaining stocks of austenitic steel from the LHC quadrupole production (Thyssen TKN).

First collaring trials have started with the assembly of a short (150 mm) mechanical model, in which the coil's straight section is replaced by stacks of cables. The mechanical model is equipped with capacitive pressure transducers that allow the evaluation of the coil compression during collaring, after collaring and at 77 K in liquid nitrogen. After the first collaring tests, small modifications were carried out to collars, collaring shoes and assembly mandrel.

The 2<sup>nd</sup> collaring test was successful. Measurements from the instrumentation indicated a compression of the coil after collaring of 40 MPa at room temperature with nominal shimming. More collaring trials with different coil shimming are scheduled over spring 2011 to determine the correct assembly parameters to reach the nominal pre-stress of 65-80 MPa, and to test the assembly at 77 K to determine the evolution of the pre-stress at cold.

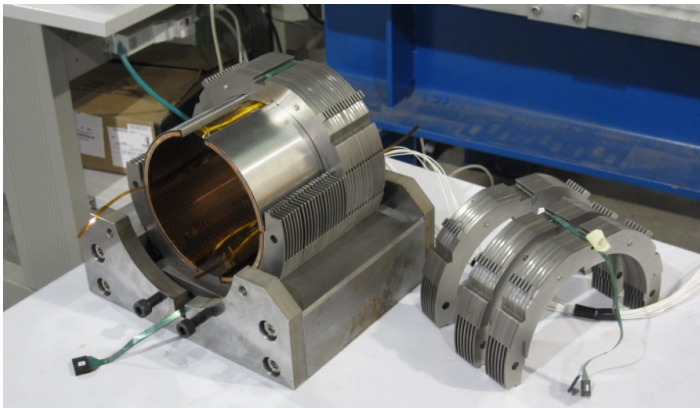


Figure 19: MCXB 150 mm mechanical model during assembly

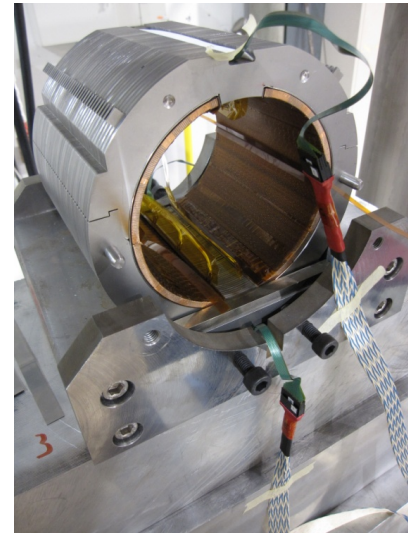


Figure 20: MCXB 150 mm mechanical model after collaring

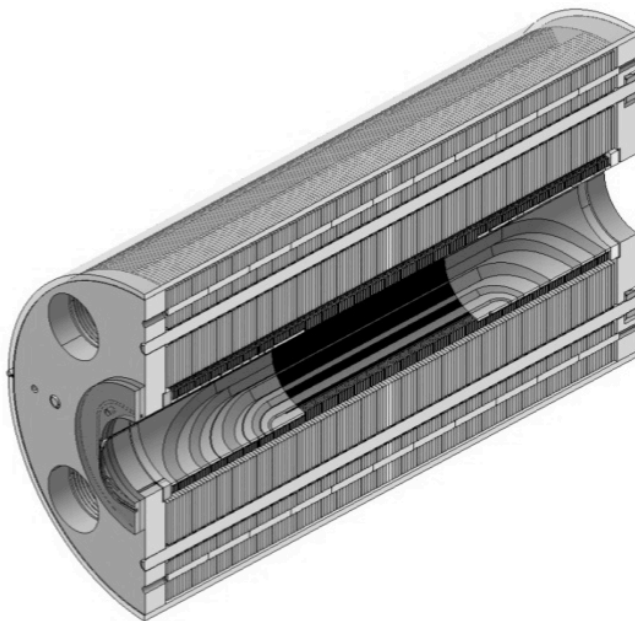


Figure 21: MCXB Magnet, 3D general assembly. Longitudinal section.



Figure 22: MCXB verification of assembly parameters on prototype parts (coil arches, collar packs and yoke laminations)

Components for the model magnet are being procured. The coil fabrication tooling for the first model is expected by end of March 2011. The assembly of the first magnet model assembled is scheduled for October 2011.

The cable for the 2nd model magnet will be insulated with a 0.1-mm-thick E-glass sleeve, directly braided around the 18-strand cable. The coils will be vacuum impregnated with an epoxy/cyanate-ester resin mix [2] to enhance radiation hardness [2]. Tests on an epoxy-impregnated stack have been carried out. The measured Young's modulus was 15.3 GPa, twice the elastic modulus measured on the polyimide version of the same stacks.

To save time and to reduce the cost of the mechanical structure for the model with potted coils re-use the same collars, laminations and instrumentation as for the model with porous insulation. Winding tooling and impregnation mold have already been manufactured. Coil winding trials should start in May 2011.

## 2.8. MCXB COMBINED H/V-CORRECTOR WITH NESTED COILS

The work on the conceptual design of the combined H/V-magnet is progressing in parallel with the construction of the model magnets variant #1 and variant #2. Figure 23 illustrates a cross-section of such a nested dipole arrangement. The detailed design will be completed after the evaluation of the first two single layer magnets, which is expected towards the end of 2011. The completion of the combined H/V-model magnet is then expected by mid 2013 taking into account all intermediate steps including parts drawings, tooling, procurement activities, mechanical model(s) etc.

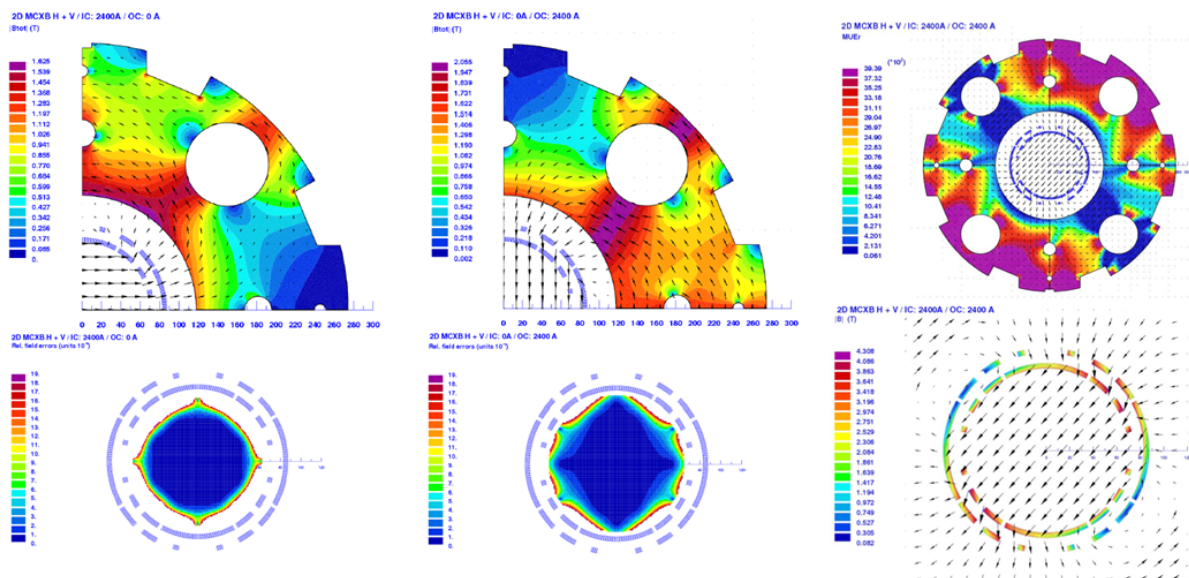


Figure 23: H/V-MCXB - Individual and combined powering of nested dipoles, flux density and saturation effects

Fig. 22 illustrates the flux density and the field quality when one dipole is powered at a time only and when both nested dipoles are powered at nominal current (from left to right: inner coil powered, outer coil powered, both coils powered). In this later case, the heavily saturated regions around the heat exchanger holes limit the field quality to  $10^{-3}$  level and lower the main field reachable by each dipole, see Fig. 24.

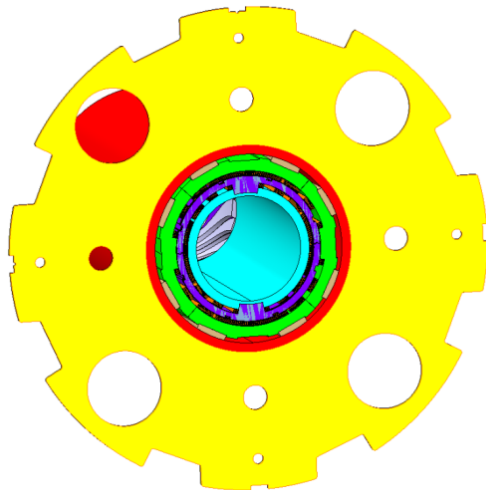


Figure 24: Possible Concept for combined H/V MCXB magnet with porous insulation

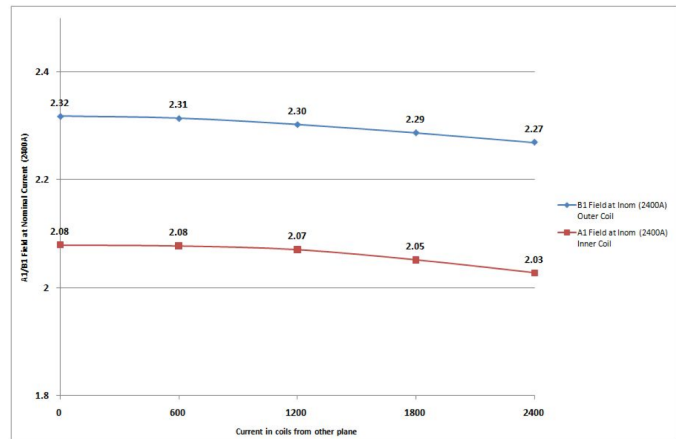


Figure 25: Combined H/V MCXB Magnet. Saturation effect on main fields during dual H+V powering

### 3. ENGINEERING DESIGN AND CONSTRUCTION WORK ON THE SEXTUPOLE AND OCTUPOLE AT CIEMAT

In the framework of the SLHC Collaboration, the CIEMAT Accelerator Technology Group has developed two superconducting prototype corrector magnets: a sextupole and an octupole. This document will describe the main steps of this work: magnetic calculations, engineering design and fabrication.

#### 3.1 CONCEPTUAL DESIGN

Table 6 summarizes the requirements for the corrector magnets performance coming from the second version of the beam optics simulations [1]. The maximum current is imposed by the existing power supplies and by the current rating of the superconducting leads. The aperture of the correctors must be equal to or larger than the aperture of the low- $\beta$  quadrupole MQXC, which is 120 mm. Studies of magnet protection from particle debris have shown that the energy deposition in the corrector package is generally higher than in the MQXC, and that the radiation dose can be reduced by a factor of two, if the aperture of the correctors is increased from 120 to 140 mm. Furthermore, as the outer diameter of the cold beam pipe is 120 mm, the free space between the cold beam pipe and the magnet allows the addition of a stainless steel tube to shield the radiation on the coils and increase the expected lifetime of the magnet.

Corrector type	Sextupole	Octupole	
Nominal current	< 120	< 120	A
Integrated strength @ 40 mm	0.055	0.035	T/m
Aperture (diameter)	140	140	mm

Table 6.: Technical specifications for corrector magnets.

Since the integrated strength of both magnets is moderate, the first choice is a superferric design. In the case of the sextupole, limiting the field to 1.4 T at the iron pole tip of 70 mm radius to avoid important saturation of the iron yoke, one gets a strength of 285 T/m<sup>2</sup>. This provides the required integrated field with an effective length of just 120 mm. In the case of the octupole, following a similar reasoning, one needs an effective length of 134 mm.

The superferric design has two important advantages:

- 1) The coils are placed beyond the clearance of the aperture and the wires are confined in a small slot, compared to the broad distribution of a cos- $\theta$  type magnet coil. Both features lead to higher radiation resistance.
- 2) The fabrication, complexity and cost is lower because the coils are flat and the wire positioning tolerance is relaxed.

The available time for the corrector magnet design and fabrication was very short (14 months), as this work could only be started after the fixing of the magnetic parameters. The

decision was to produce the sextupole following the conventional techniques for superferric accelerator magnets and concentrate the efforts on the design and fabrication of a sextupole magnet with high radiation resistance.

### 3.2 Magnetic design

First step of the magnetic calculation is the cross section optimization, performed with ROXIE, a computing tool developed at CERN for the design of superconducting magnets. In the case of a superferric magnet, the field shape at the aperture is provided by the iron pole profile, as stated by the Maxwell laws. The equation of that profile for a sextupole reads in Cartesian coordinates:

$$3x^2y - y^3 = \pm R^3 \tag{1}$$

where R is the aperture radius. As this curve is not directly available in ROXIE, it has been approximated using five circular arcs and a straight line in the proximity of the coil. Table 7 summarizes the main results of the magnetic optimization for the sextupole cross section. The superconducting wire is provided by Supercon. The filament diameter is very small to avoid magnetization effects due to persistent currents. The iron peak field is kept relatively small to decrease the nonlinearity of the transfer function. Figure 26 depicts the magnetic field map in the iron yoke at nominal current.

Corrector type	Sextupole	
Nominal current	100	A
Bare wire diameter	0.5	mm
Insulation thickness	0.02	mm
Cu/Sc	1.55	
Filament size	4	μm
Number of turns	228	
Gradient	250.15	T/m <sup>2</sup>
Reference radius	40	mm
Nominal field	0.4	T
b9	-0.010	1e-4
b15	0.0035	1e-4
b21	0	1e-4
Non-linearity in the load line	0.1	%
Coil peak field	2.02	T
Working point @ 1.9 K	33.5	%
Iron outer radius	140	mm
Self inductance	1.40	H/m
Stored magnetic energy	7.02	kJ/m

Table 7: 2D magnetic computation results for the sextupole.

Next step of the magnetic calculation is the full model in 3D. Since the magnet length is similar to the aperture, the coil end contribution is very significant for the integrated field value, and the full modelling is unavoidable. ROXIE has been also used for this computation. Table III summarizes the results after harmonics optimization. The aim is to keep the magnet as short as possible, because it is very advantageous for the near subsystems. But the coil ends are not placed very close to the iron yoke to avoid the saturation of the iron pole tip and, therefore, the increase of the field harmonics and the nonlinearity of the transfer function.

|Btot| (T)  
Time (s) : 1.

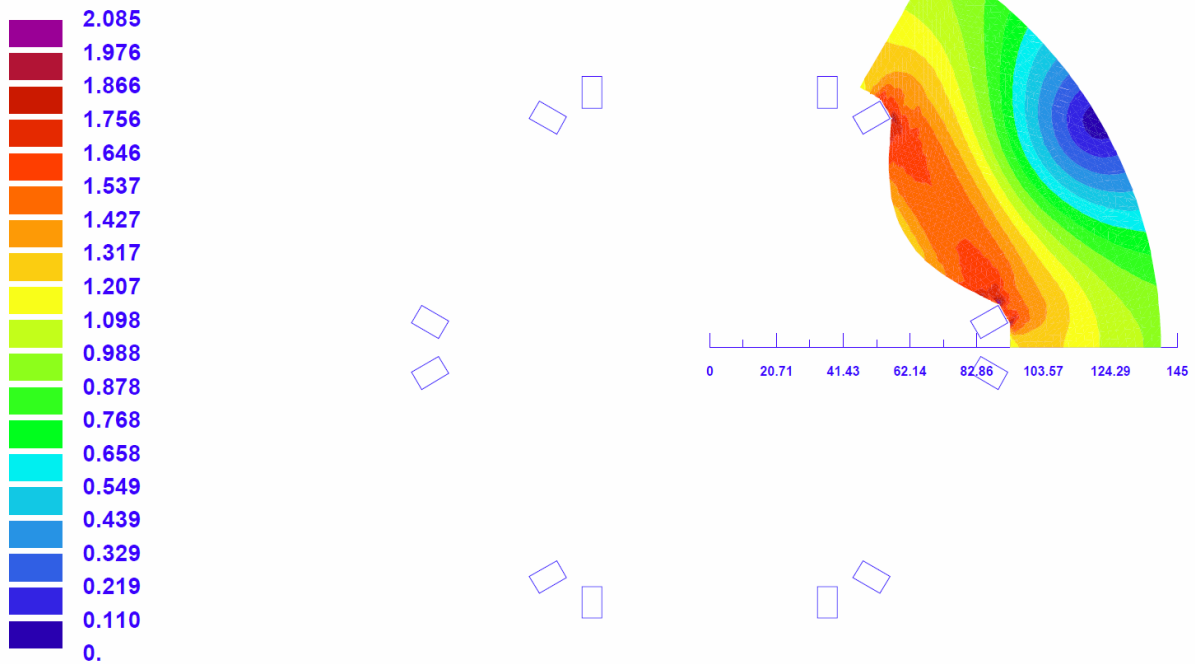


Figure 26: 2D magnetic field map in the iron yoke at nominal current (computation performed with ROXIE).

The yoke is made of pure iron, which guarantees a high saturation magnetization. The nonlinearity is about 3%, which is understood as non-problematic for the machine operation. A further decrease of the nonlinearity would yield a longer magnet. Another consequence of the coil end geometry is that the peak field is still at the coil straight section, not at the ends, where a peak field enhancement usually takes place. The working point on the load line is low. As the stored energy is relatively low, this magnet will have a good behaviour in case of a quench.

Nominal current	100	A
Bare wire diameter	0.5	mm
Insulation thickness	0.02	mm
Cu/Sc	1.55	
Filament size	4	$\mu\text{m}$
Number of turns	228	
Effective length	0.137	m
Overall length	160	mm
Integrated strength	0.055	T.m
Integrated b9	0.504	1e-4
Integrated b15	0.127	1e-4
Integrated b21	-0.001	1e-4
Non-linearity in the load line	3	%
Coil peak field	2.02	T
Working point @ 1.9 K	33.5	%
Iron outer radius	140	mm
Self inductance	192	mH
Stored magnetic energy	960	J

Table 8: 3D magnetic computation results for the corrector sextupole.

Figure 27 depicts the magnetic field profile at the reference radius, along a line parallel to the magnet axis. It must be noticed that the field is not constant in the straight section of the magnet, due to its short length, compared to the aperture.

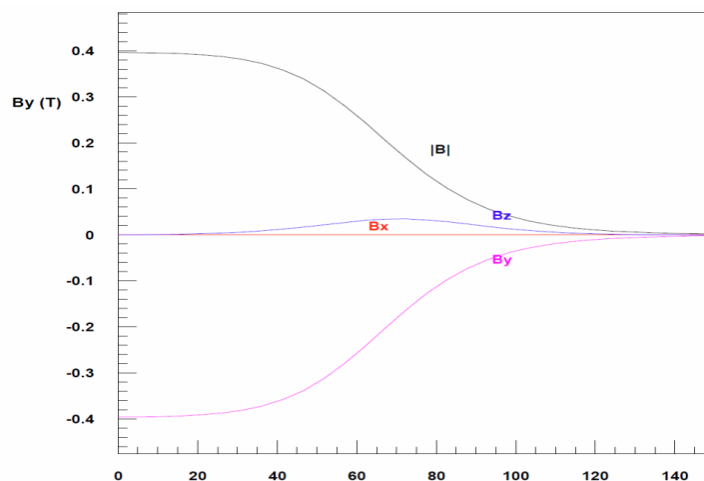


Figure 27: Magnetic field profile along the axis, at  $r = 40$  mm, only half magnet is shown. Horizontal axis shows the distance from the magnet center in mm (computation performed with ROXIE [6]).

Figure 28 shows the field map in the iron yoke; notice the field enhancement at the iron pole, especially close to the wires.

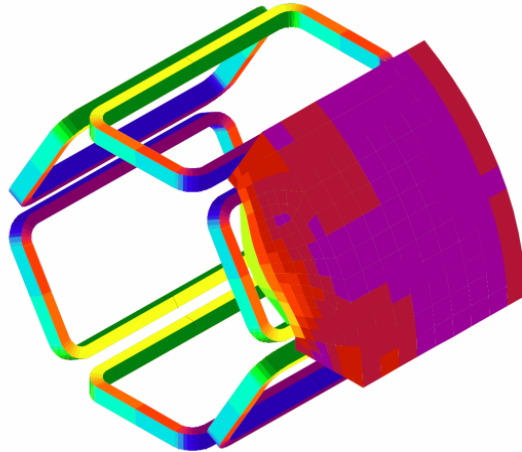


Figure 28: 3D magnetic field map in the iron yoke at nominal current, colours at coils show the current density values (computation performed with ROXIE).

For the octupole magnet, the design methodology is very similar to the sextupole magnet described above. The iron pole profile should be an equipotential line to provide an octupole field map in the aperture. It is given by the equation:

$$x^3y - xy^3 = \pm R^4 \tag{2}$$

As it was explained for the sextupole, that line has been approximated using five circular arcs and a straight line. Due to the large impact of the coil ends on the integral field in these short magnets, the magnetic calculation was directly done in 3D. Table 9 shows the main results of the optimization. The superconducting wire is also chosen from standard material produced by Supercon. The iron yoke is made of pure iron.

Nominal current	100	A
Bare wire diameter	0.5	mm
Insulation thickness	0.02	mm
Cu/Sc	1.5	
Filament size	5	μm
Number of turns	165	
Effective length	0.161	m
Reference radius	40	mm
Integrated strength	0.035	T.m
Integrated b12	0.052	1e-4
Integrated b20	0.016	1e-4

Integrated b28	-0.001	1e-4
Non-linearity in the load line	2.2	%
Coil peak field	1.87	T
Working point @ 1.9 K	30.6	%
Iron outer radius	125	mm
Self inductance	152	mH
Stored magnetic energy	758	J
Overall length	180	mm

Table 9: 3D magnetic computation results for the corrector octupole.

Figure 29 shows the magnetic field profile along a line parallel to the magnet axis, in the horizontal plane, at  $r = 40$  mm. Since the octupole is slightly longer than the sextupole, the field is more uniform in the central section of the magnet. Figure 30 illustrates the magnetic field map in the iron yoke.

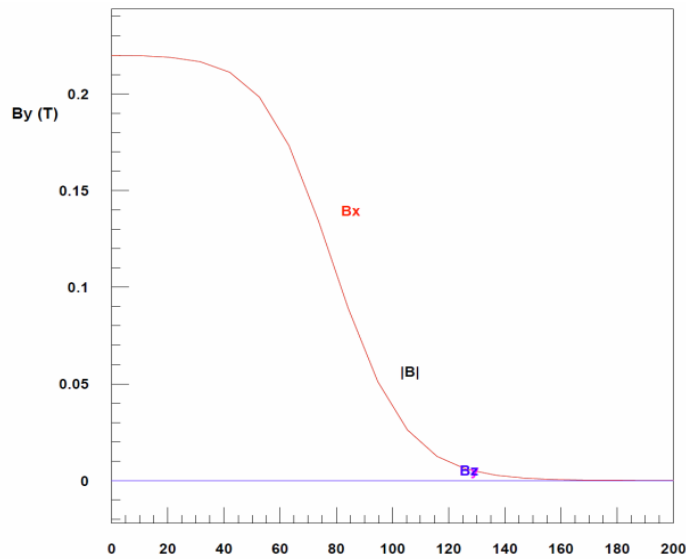


Figure 29. Magnetic field profile along the axis, at  $r = 40$  mm, only half magnet is shown. Horizontal axis shows the distance from the magnet center in mm (computation performed with ROXIE).

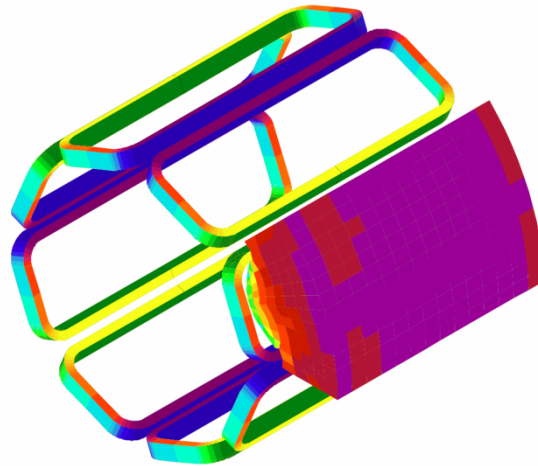


Figure 30: 3D magnetic field map in the iron yoke at nominal current, colours at coils show the current density values (computation performed with ROXIE [6]).

### 3.3 Engineering design

Standard techniques are used for the sextupole engineering design [7]. The coils will be wet impregnated during the winding with standard Araldite epoxy resin (AW106 resin with HV953U hardener). Figure 31 (left) shows the 3D model of the mould. The winding mandrel is made in aluminium and later extracted by immersion in a liquid nitrogen bath. The right shape of coils is guaranteed by external clamps which pressure T-shaped keys on the coil sides.

Figure 31 (right) shows the rendering of an assembled magnet. The iron yoke is made of laminations of 4 mm thickness, cut by EDM, which guarantees, for small quantities, a good accuracy with a reasonable price. The laminations are packed using long threaded rods, made of steel to match the contraction coefficient of the iron yoke, and two thick stainless steel (non magnetic grade) plates at both ends. The alignment is provided by outer stainless steel keys, which will be also used for the alignment of the magnet into the support structure of the cryostat and for mechanical reference to measure the field harmonics.

The coils are supported at the end spacers, using screws to link them with the yoke endplates. Moreover, stainless steel wedges are placed in between two coils, to support them when they are energized, when the magnetic forces tend to pull out the coil straight section. All the coil parts in contact with metallic surfaces are insulated with G11 sheets (0.2 mm thick). Additionally, the straight part of the coils is surrounded by two layers of adhesive polyimide tape for increased protection.

The connections are made with conventional soldering over a minimum length of 40 mm, to minimize the electrical contact resistance. The wires are stabilized with thin electrolytic copper ribs (2x3 mm) to provide additional margin to quench. Once the wires are soldered, they are fixed into a G11 connection plate with Stycast 2850FT epoxy resin to avoid any movement. The current leads are stabilized with a superconducting wire in parallel, soldered each 150 mm, and insulated with fibreglass sleeves impregnated with silicon.

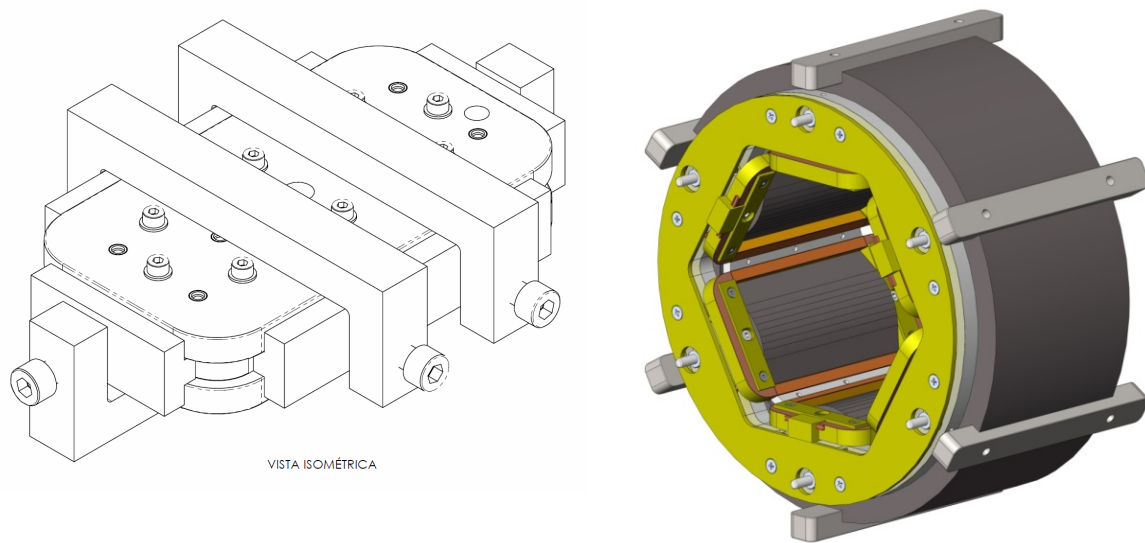


Fig. 31: Left: Rendering of impregnation mould with clamping for curing. Right: Rendering of assembled magnet.

The octupole shall be hard-radiation resistant. Here we concentrate on the main differences in design methodology with respect to the sextupole.

The resin will be a cyanate ester, with reference 422-B, produced by Compound Technology Development, Inc., which shows very good performance under a radiation dose of the order of 10 MGy. The impregnation will be done under vacuum, because the viscosity of the resin is very low. The resin must be outgassed prior to be introduced into the mould. The curing cycle is relatively long and delicate, because the mixture is exothermic. The mould is depicted in Figure 32 (left). It will be made of stainless steel. A new vacuum chamber has been designed, where the mould will be introduced, which allows to relax the tightness requirement of the impregnation mould: it only needs to be liquid tight. The mould is closed using Viton elements (O-rings, wires and sheets), which can withstand the curing temperature without degradation.

The coil end spacers are made of stainless steel instead of standard G11 ones. A polyimide sheet guarantees the electrical insulation to the wires. Several materials (polyimide, cyanate-ester fibreglass composite) are considered.

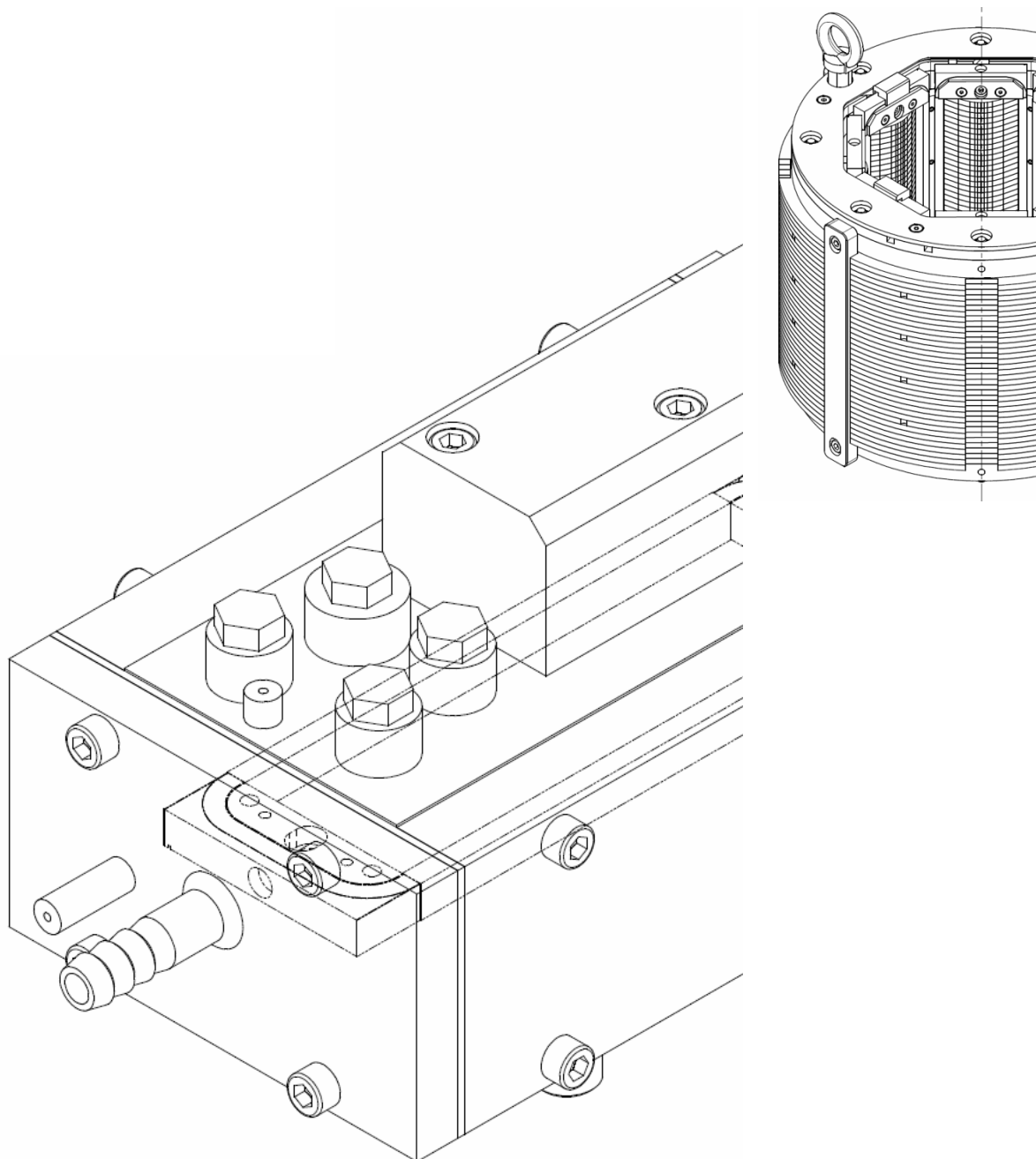


Figure 32: Left: Drawing of impregnation mould. Right: Drawing of assembled magnet.

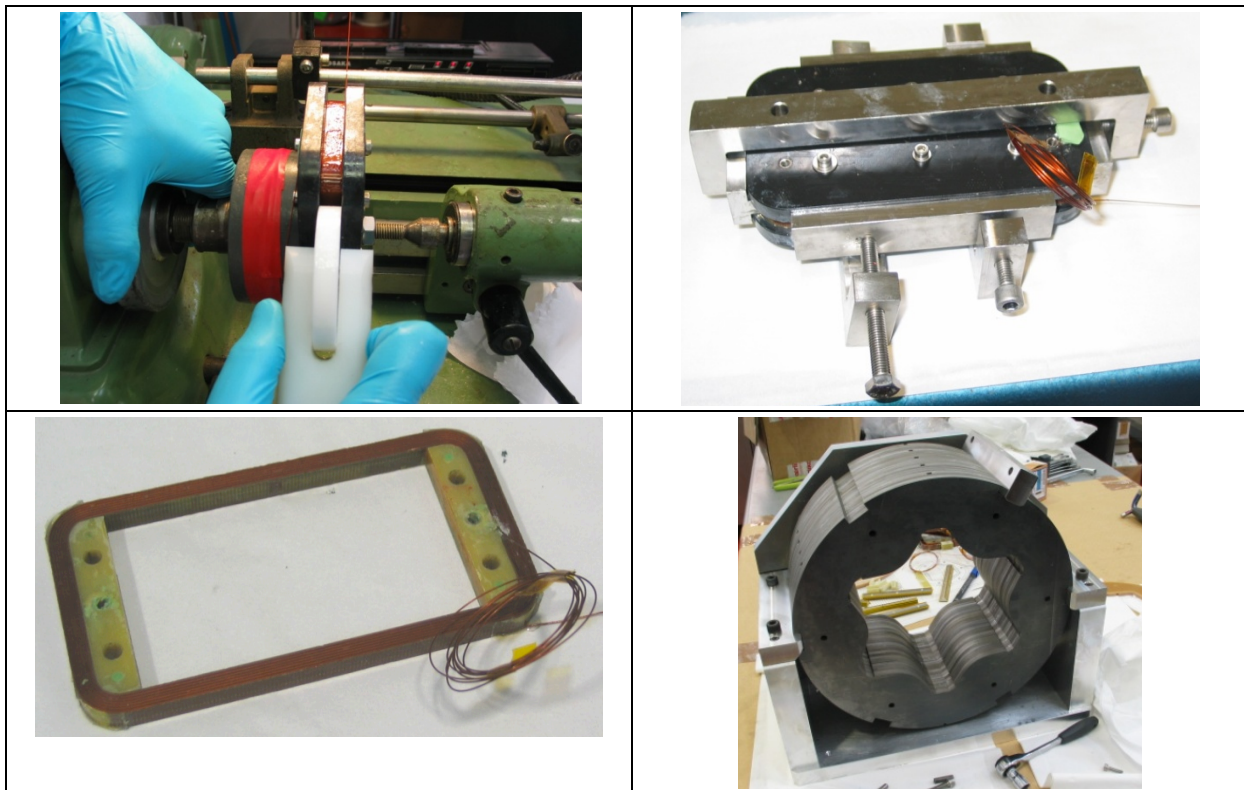
### 3.4 Fabrication

Due to the late start of the engineering design stage, caused by delays after the LHC incident and the recalculation of the Upgrade Phase I beam optics, only the sextupole magnet has been finished. In the case of the octupole, the impregnation mould has been fabricated and

magnet components have been procured. CIEMAT and CERN are fully committed to finish the construction and cold testing of this magnet, to make best use of the investments.

Figure 8 shows the main stages of the magnet fabrication: coil winding, de-moulding, iron laminations packaging, connection soldering and final magnet assembly.

Table 9 summarizes the dimensional control on the fabricated coils (one spare), which are quite repetitive and close to nominal values. Figure 32 shows the dimension references. Table 10 shows the electrical measurements (self-inductance at two different frequencies and resistance), which proof that there are no short-circuits. Besides, the ground insulation has been checked by applying 500 V with a capacitor discharge.



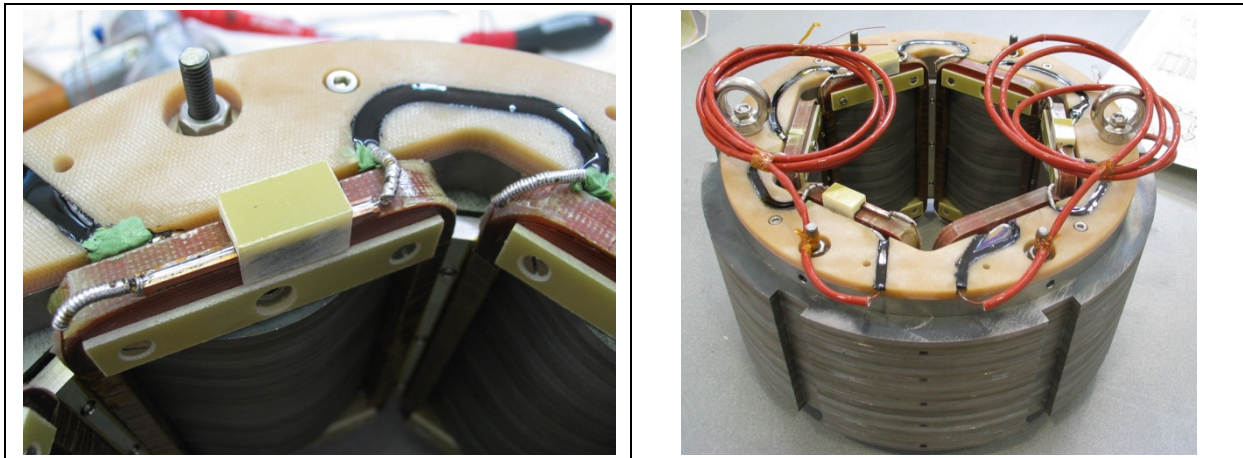


Figure 33. Upper left: a complete layer of wires is positioned in the coil winding machine. Up right: the mould is closed and ready for curing. Middle left: the coil is finished but not insulated with polyimide tape wrapped around. Middle right: the iron laminations are being packed. Lower left: connections are being fixed into the connection plate with epoxy resin. Lower right: finished magnet with insulated current leads.

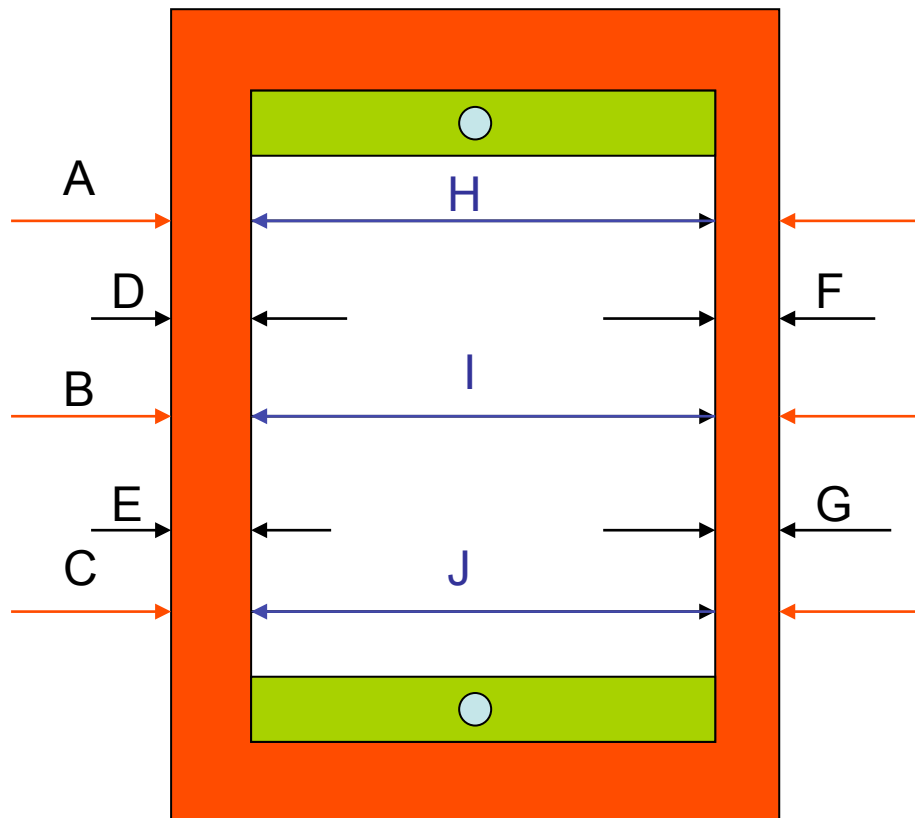


Figure 34. Dimension references for Table 9.

Reference	A	B	C	D	E	F	G	H	I	J
Nominal	79.92	79.92	79.92	6.91	6.91	6.91	6.91	66.11	66.11	66.11

Coil 1	80.07	80.13	80.18	6.91	6.95	6.88	6.87	66.22	66.28	66.24
Coil 2	80.26	80.42	80.52	6.96	6.95	6.98	6.74	66.88	66.46	66.62
Coil 3	80.18	80.20	80.09	6.98	7.10	7.05	7.26	66.21	66.43	66.21
Coil 4	80.20	80.15	80.10	6.92	6.92	6.95	6.98	66.20	66.15	66.20
Coil 5	80.33	80.55	80.55	7.05	7.08	6.96	6.93	66.16	66.14	66.07
Coil 6	80.23	80.19	80.22	6.95	6.89	7.08	7.18	66.28	66.15	66.09
Coil 7	80.09	80.1	80.15	7.03	6.99	6.98	7.02	66.03	66.18	66.1
Average	80.22	80.28	80.31	7.01	6.99	7.01	7.04	66.16	66.16	66.09
Std. Dev.	0.18	0.26	0.26	0.07	0.09	0.07	0.12	0.10	0.03	0.02

Table 10: Dimensional control of the sextupole coils (insulated). Measurements given in mm.

	Self-inductance (mH, 100 Hz)	Self-inductance (mH, 1 kHz)	Resistance (ohm)
Coil 1	11.629	11.621	13.729
Coil 2	11.633	11.625	13.809
Coil 3	11.642	11.635	13.763
Coil 4	11.651	11.643	13.826
Coil 5	11.641	11.634	13.813
Coil 6	11.643	11.634	13.756
Coil 7	11.631	11.623	13.815
Average	11.64	11.63	13.79
Std. Dev.	0.01	0.01	0.03

Table 11: Electrical measurements on the sextupole coils.

### 3.5 Cold testing

The magnets will be tested at CIEMAT's cryogenic test facility. A new insert with lower thermal losses is under preparation for an existing vertical cryostat, whose diameter is 310 mm and length is 1532 mm. A new data acquisition system has been developed, based on an Agilent 64-channel card, which allows up to 500 kHz frequency acquisition, divided by the number of active channels; see Fig. 10. As the peak voltage of the card is 10 V, which is much lower than the voltage signals to measure, eleven custom cards have been developed to adapt the voltage levels. Four different levels of peak voltage may be chosen (250, 500, 750 or 1000 V). All the channel inputs are differential and able to withstand up to 1500 V in common mode. These cards have different configuration for low or high resolution, depending on the input voltage value. In the low resolution mode, noise is below 0.5% and in the high resolution mode below 0.1%. The magnet training tests will be performed in the first half of 2011.

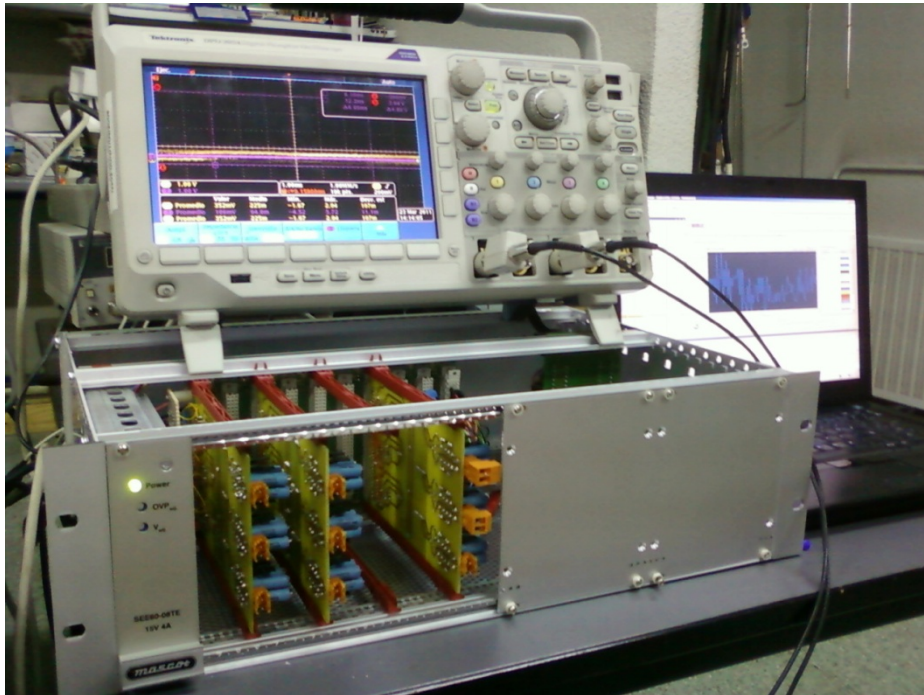
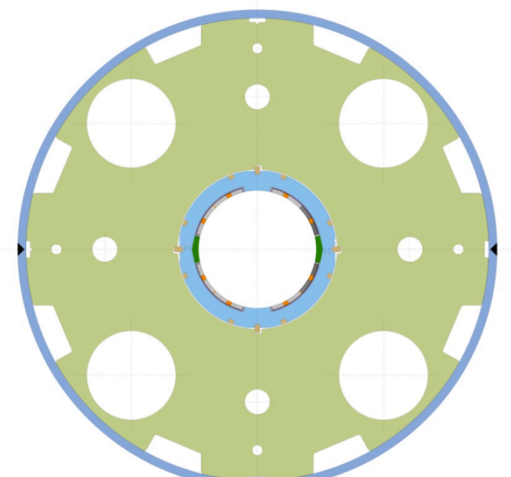


Figure 35. Data acquisition system for superconducting magnet test station.

#### 4. CONCEPTUAL AND ENGINEERING DESIGN FOR THE SKEW QUADRUPOLE

As for the MCXB dipole correctors, the requirements for the MQXS Skew quadrupoles have been revised in 2009. Table 62 lists the initial and actual design parameters for the MQXS skew quadrupoles. The design is based on collared coils using the same 18-strand Rutherford-type cable with porous polyimide insulation as for the MCXB magnets.

Nominal Gradient	25.5	T/m	(40 T/m)
Magnetic length	0.64	m	(0.5 m)
Nominal current	2400	A	(1602 A)
Stored energy	8.8	kJ	(19.1 kJ)



Self inductance	3.0	mH	(15 mH)
Working point	44	%	(55 %)
Cable width	4.37 mm		(3.40 mm)
Cable mid-height	0.845 mm		(0.845 mm)
Total length	900	mm	(800 mm)
Aperture	140	mm	(140 mm)
Total mass	500	kg	(500 kg)

Table 62: MQXS Design Parameters (initial parameters in brackets)

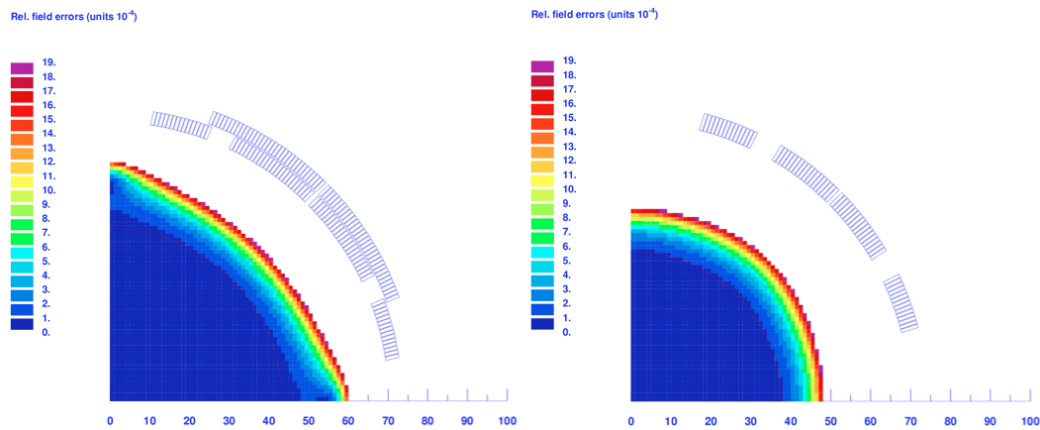


Figure 37: MQXS 2D Field Quality: 40 T/m two layer design, and the actual 25.5 T/m single layer design

#### 4.1. MAGNETIC DESIGN OF THE MQXS (SINGLE LAYER 2 BLOCKS DESIGN)

The magnetic design (2D and 3D) has been carried out at CERN, using ROXIE [6]. The 32 turns of the single-layer coil are grouped in 2 winding blocks of 18 and 14 turns.

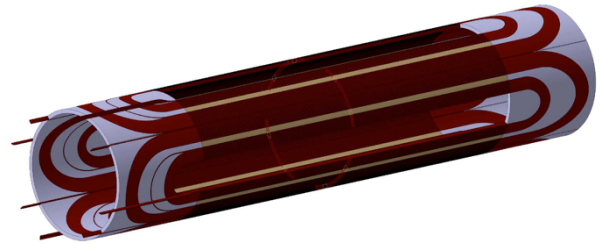
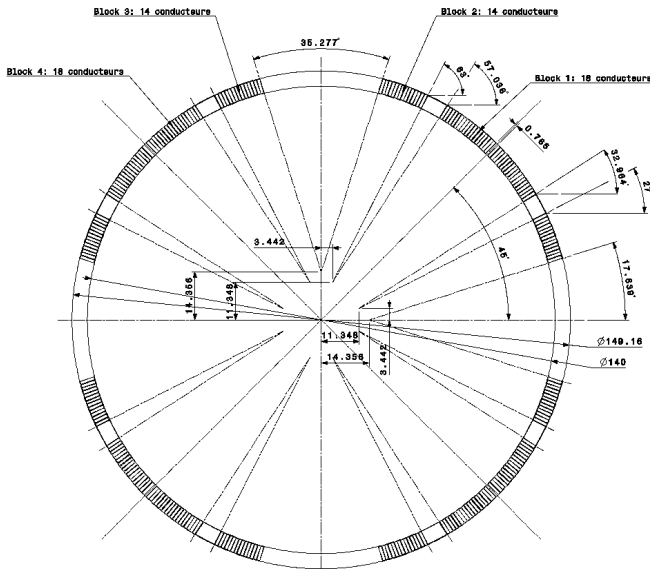


Figure 39: MQXS 3D view of the coils

Figure 38: MQXS 4 coils cross-section

<b>Contribution to <math>A_2</math></b>	Length	Integrated Field
Straight section	470 mm	1.02 Tm
Return End	120 mm	0.087 Tm
Lead End	120 mm	0.087 Tm
<b>Total</b>	<b>710 mm</b>	<b>0.65 Tm</b>

<b>3D Harmonics at 2.4 kA (units)</b>			
$A_2$	0.65 Tm	$b_2$	19.59
$a_6$	0.04	$b_6$	0.49
$a_{10}$	0.25	$b_{10}$	-0.08
$a_{14}$	-1.37	$b_{14}$	-0.01

Table 13: Magnetic lengths and integrated 2D field harmonics

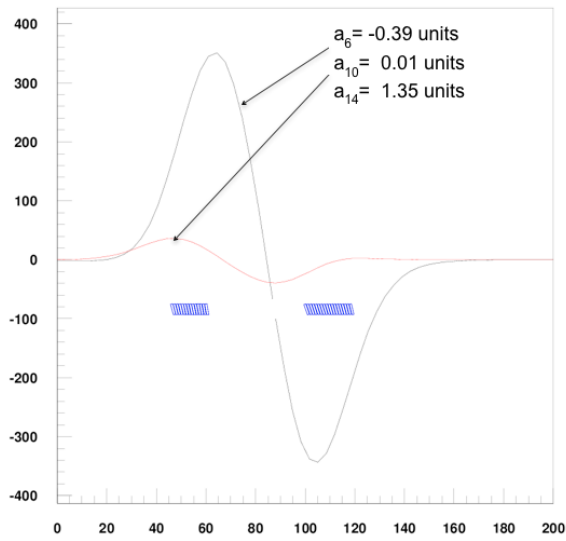


Figure 40: 3D computation of field harmonics (MQXS Return End)

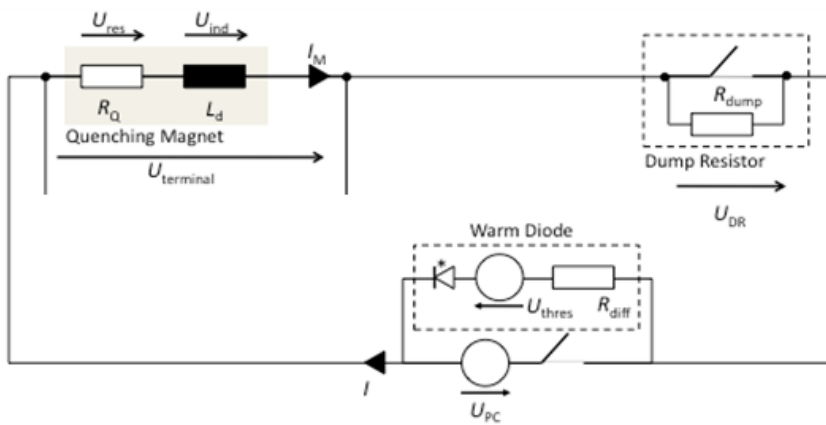


Figure 41: MQXS Energy Extraction Scheme

As for the MCXB dipole correctors, the limited stored energy in the MQXS magnet allows for a simplified quench protection scheme. Simulations have shown that an energy extraction system based on a warm by-pass diode and a 0.16 Ohm dump resistor is sufficient to protect the magnet and no quench heaters are required.

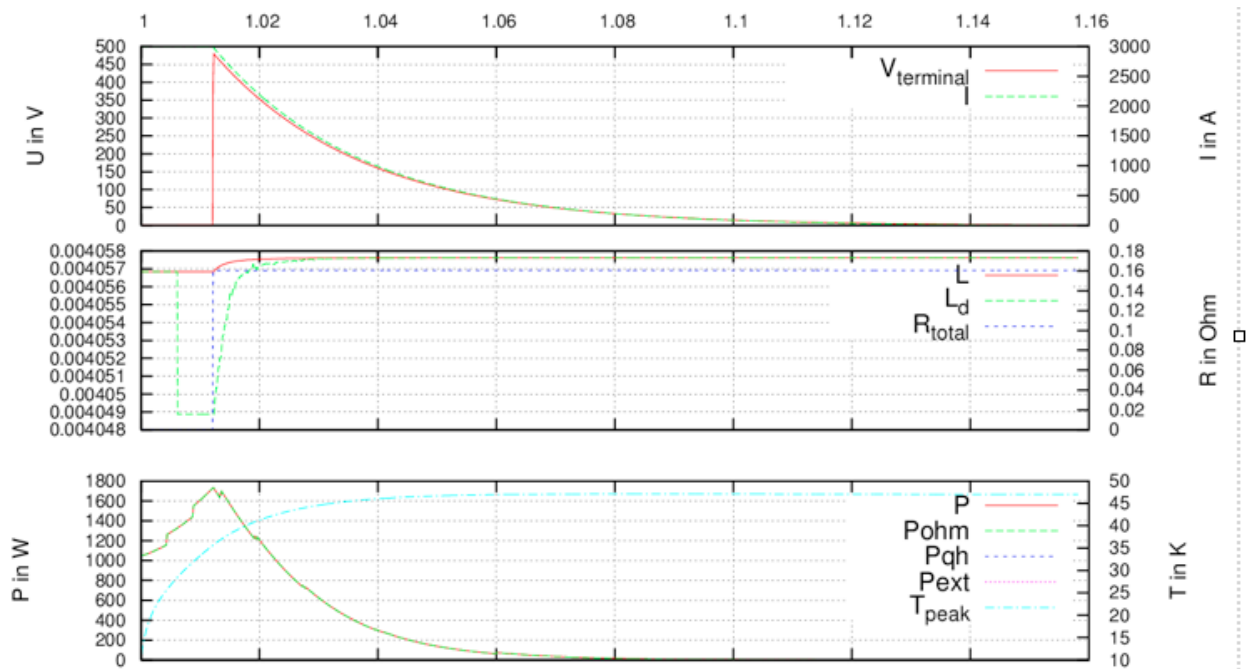


Figure 42: MQXS quench computation. Voltage, inductance, and power dissipation

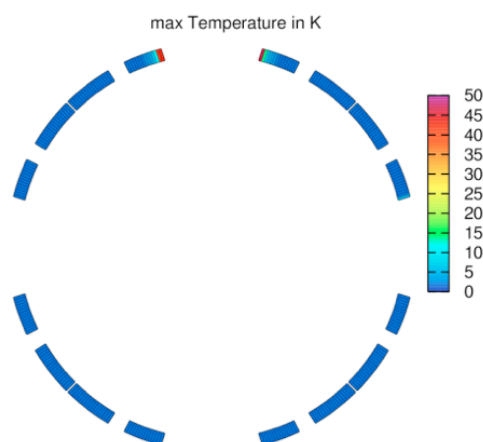


Figure 43: Temperature profile during quench

### 4.2. FINITE ELEMENT STRUCTURAL ANALYSIS

Structural Analysis of the MQXS model has been carried out at CERN using ANSYS. The 2D cross-section of the collared coils was used to assess the deformation and stress in the collars, as well as the evolution of the azimuthal compression in the coil during collaring, cool down, and when the magnet is powered. The electro-magnetic simulation in Ansys® agrees with ROXIE results. Under magnetic forces the azimuthal compression of the coils decreases

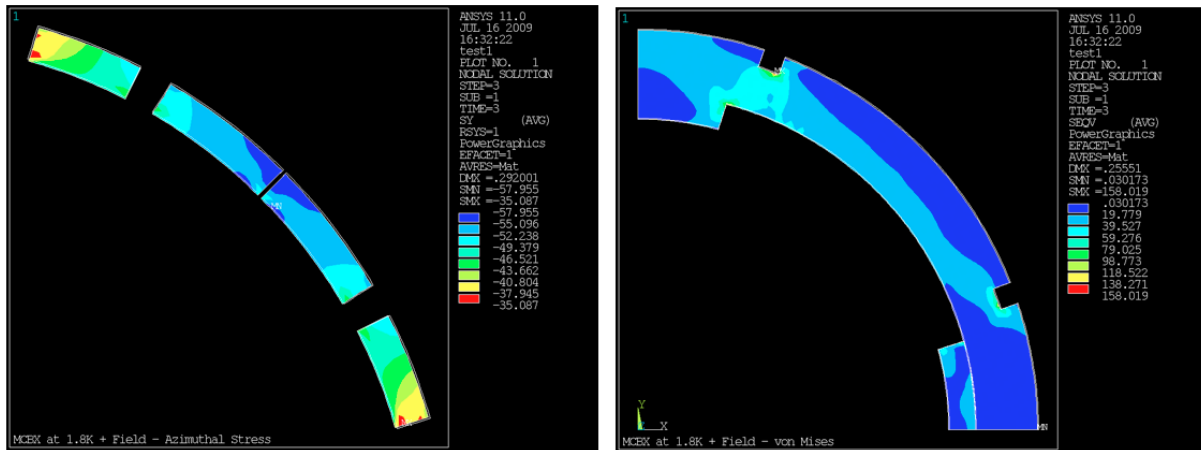


Figure 44: MQXS azimuthal stress distribution in the coil at nominal current and Von Mises stress in the collars

at the pole, and increases at the mid-plane. The graph represents the evolution of the azimuthal compression of the coil at the pole and at the 45 deg. plane for the different stages of the magnet assembly, at 1.9 K, and during excitation.

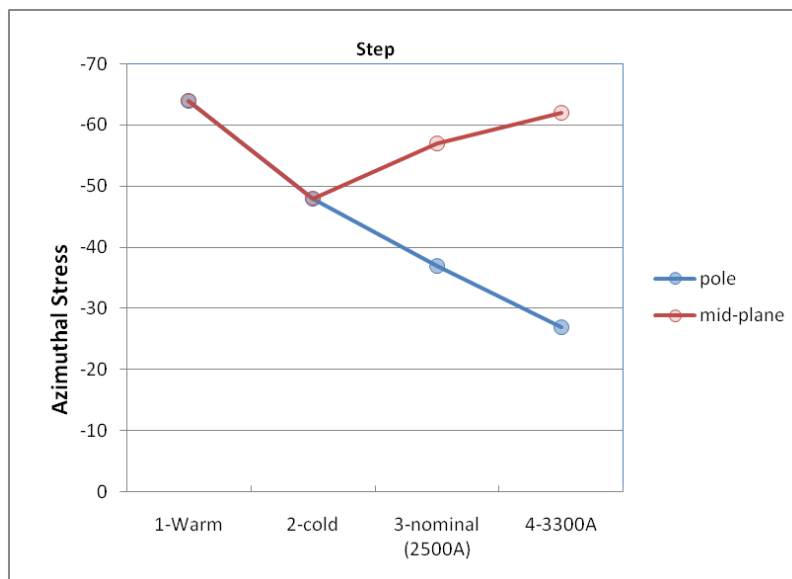


Figure 45: Evolution of the azimuthal compression in the coil at the pole and at the mid-plane during assembly, at 1.9 K, and under powering at nominal and critical current

After the re-scoping of the WP-6 in Spring 2010, the conceptual design of the MQXS skew quadrupole was completed and the construction of the model magnet was adjourned.

The entire MQXS magnet has been modelled in 3D under CATIA/smarteam CAD/PLM system. A trial coil has been wound and cured with metallic end spacers. All parts for the assembly of the 150 mm mechanical model have been procured.

## 5. CONCLUSIONS

Two superconducting corrector magnets (a sextupole and an octupole) have been developed at CIEMAT in the framework of the SLHC collaboration. Both magnets are superferric, due to the moderate peak field, low fabrication complexity and the good performance of that configuration in a hard radiation environment. The magnetic calculations have been realized with ROXIE. 3D modelling is necessary due to the short magnet length in comparison with the aperture diameter. Sextupole fabrication has been completed using standard techniques, while the octupole has innovative features to increase the magnet lifetime under radiation.

A new insert for the vertical cryostat is being fabricated, and a new data acquisition system has been developed. Cold test of the sextupole magnet will be done in the first half of 2011.

In parallel, work at CERN has aimed at the design and manufacture of orbit corrector magnets with Rutherford type superconducting cable. All tooling and magnet components have been procured from European Industry. First assembly tests have been made successfully. Moreover, the design of a skew quadrupole magnet has been completed.

## 6. REFERENCES

- [1] R. Ostojic et al.: Conceptual Design of the LHC Interactions Region Upgrade Phase-I, LHC Project Report 1163, 2008.
- [2] S. D. Grandlienard, S.W. Feucht, P.E. Fabian, D. Codell, N.A. Munsh: Properties of Cyanate-Ester-Based Composite Insulation for Magnet Applications, Advances in Cryogenic Engineering, AIP Conference Proceedings, 2006.
- [3] M. Karppinen: Corrector magnets for the LHC IR upgrade phase-1, SLHC-IRP1-MCX-ES-00001, edms doc. 1039976
- [4] S. Fartoukh, R. Tomas, R., J. Miles: Specification of the closed orbit corrector magnets for the new inner triplets, sLHC Project Report 030, 2009
- [5] N. Elias, CERN TE-MS, 2010, private communication.



## DELIVERABLE REPORT

Doc. Identifier:  
**SLHC-PP-D6.3.1**

Date: 30/03/2011

- 
- [6] ROXIE software for the electromagnetic simulation and optimization of accelerator magnets. <https://espace.cern.ch/ROXIE>; contact B. Auchmann, CERN TE-MSC.
  - [7] F. Toral et al.: Design and Fabrication of a Combined Superconducting Magnet for XFEL, European Particle Accelerator Conference, Edinburgh, 2006
  - [8] F. Cerutti, M. Mereghetti, E. Wildner: Update of Power Deposition Studies in the LHC Upgrade Phase I Insertion Regions, CERN EDMS 975134, Geneva, 2008